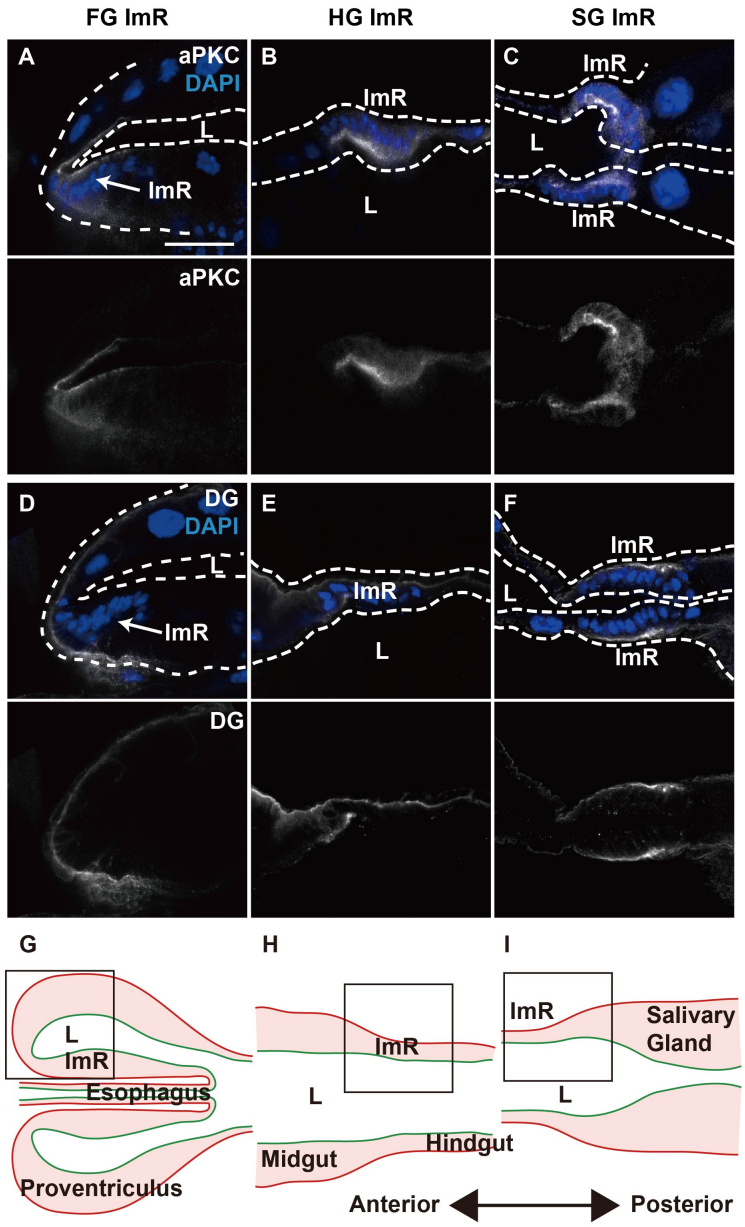

Fig. S1. The cell polarity of imaginal ring tissue at third instar larval stage.

(A-C) The apical side of the imaginal ring is marked by aPKC (white). (D-F) The basal side is labeled by DG (white). Nuclei were stained with DAPI (blue). (A and D) foregut imaginal ring; (B and E) hindgut imaginal ring; (C and F) salivary gland imaginal ring. Arrows point to imaginal ring cells. L, lumen. Scale bar, 20μm. (G-L) The cross-section of imaginal ring. Green lines for apical side and red lines for basal side. Boxes indicate the areas presented in above figures.

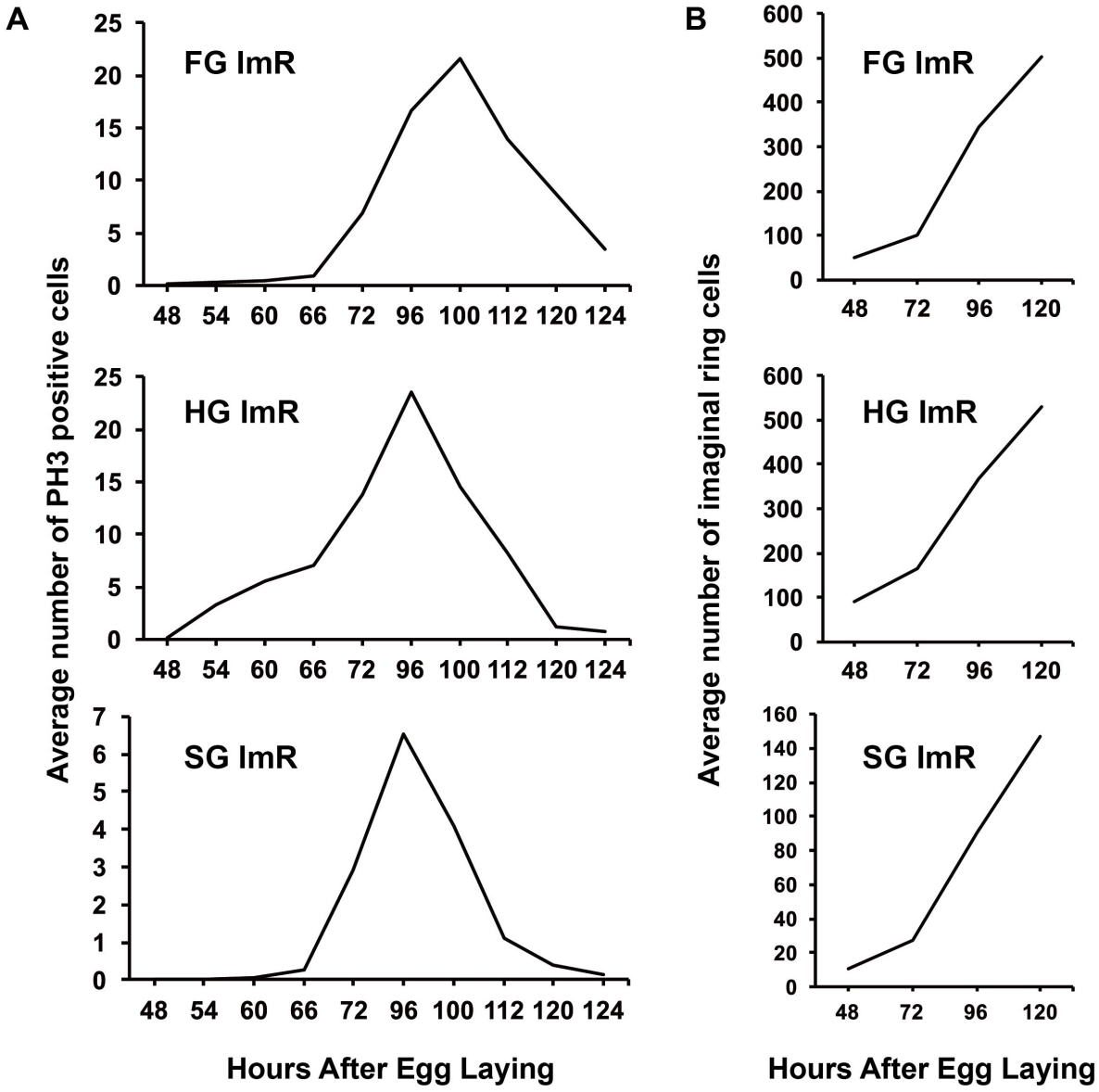

Fig. S2. The proliferation pattern of imaginal ring through larval development.

(A) Quantification of PH3 positive imaginal ring cells through 48 hours to 124 hours AEL. (B) Quantification of imaginal ring cell number at 48, 72. 96, 120 hours AEL.

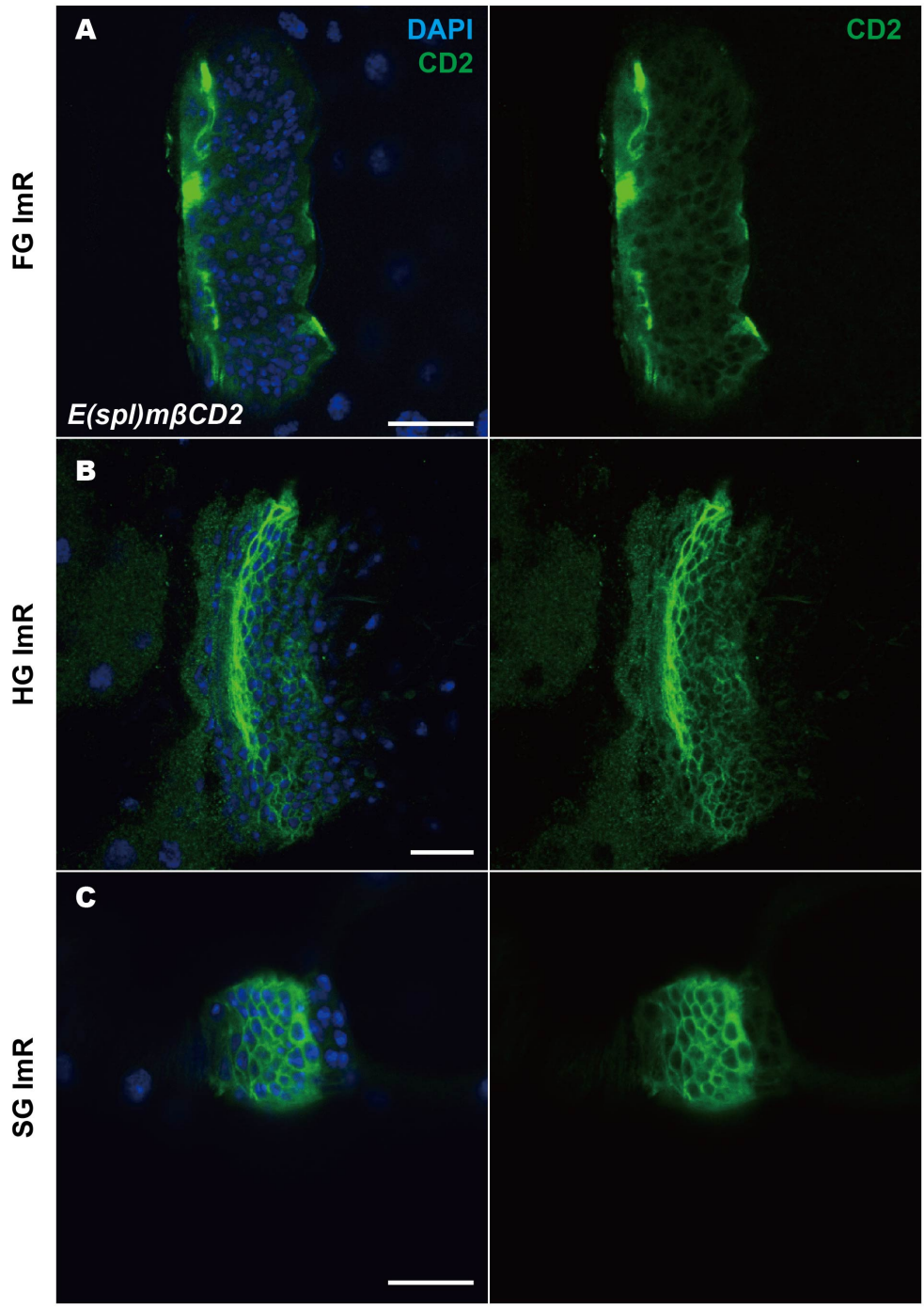

Fig. S3. *E(Spl)mβ-CD2* expression in imaginal ring.

E(Spl)mβ-CD2 expression in imaginal ring cells also showed Non-uniform expression pattern as the expressions of *NRE-eGFP* in foregut imaginal ring (A), hindgut imaginal ring (B) and salivary gland imaginal ring (C) at third instar larvae. CD2 antibody staining (green). Nuclei were labeled with DAPI (blue). Scale bar, 20μm.

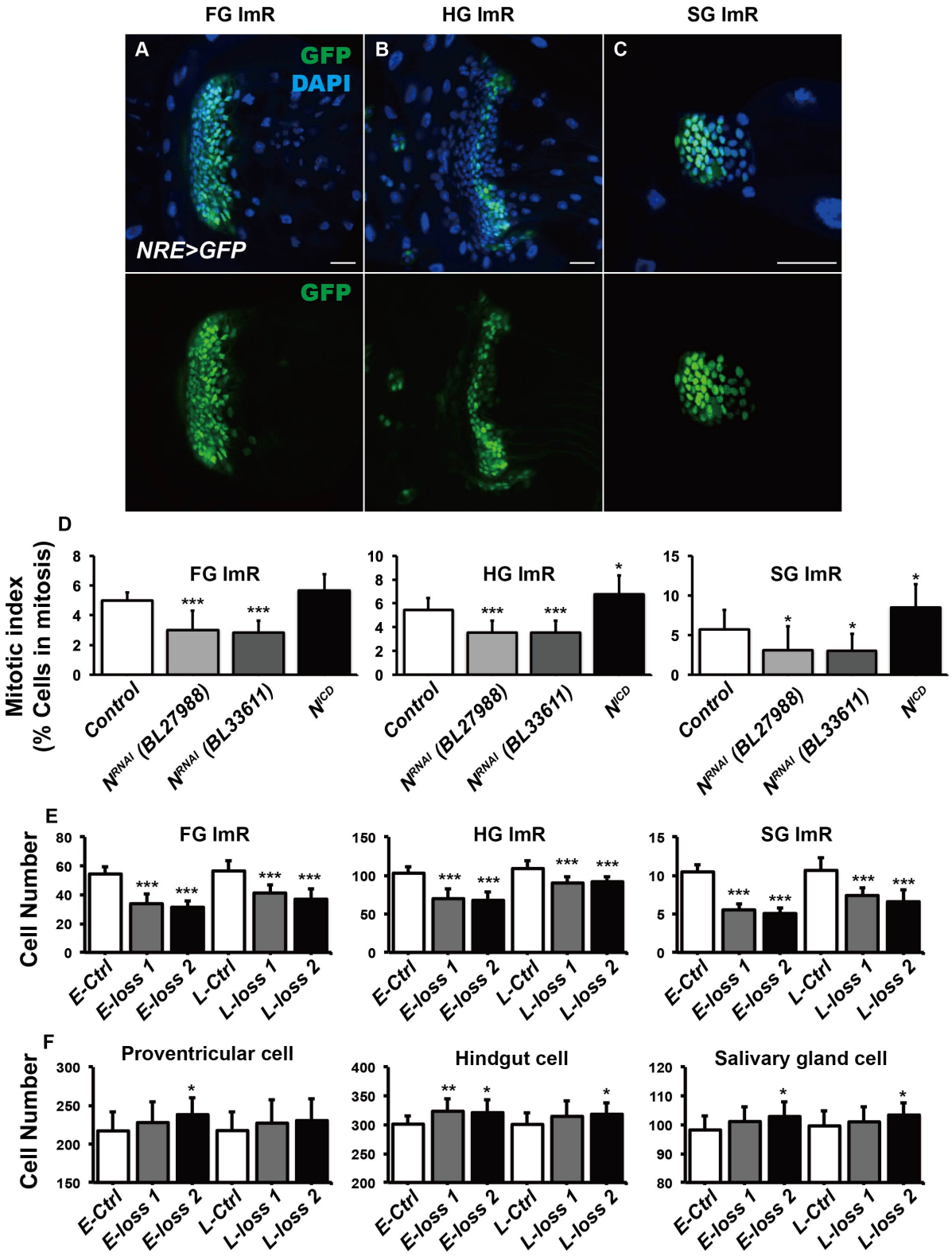

Fig. S4. *NRE-Gal4* driver applied experiments.

(A-C) *NRE-Gal4* driven GFP expression (green) in foregut imaginal ring (A), hindgut imaginal ring (B) and salivary gland imaginal ring (C) in third instar. Nuclei were labeled with DAPI (blue). Scale

bar, 20μm. (D) Quantification of mitotic index in third instar. ***, P<0.001. Error bars, mean±S.E.M. (E and F) Quantification for cell numbers in early-second instar. E-Ctrl, embryonic control; E-loss 1, embryonic loss of *Notch* by *Notch-RNAi* (BL27988); E-loss 2, embryonic loss of Notch by *Notch-RNAi* (BL33611); L-Ctrl, Larval control; L-loss 1, larval loss of *Notch* by *Notch-RNAi* (BL27988); L-loss 2, larval loss of *Notch* by *Notch-RNAi* (BL33611). Embryonic experimental design was based on Fig. S12A; Larval experimental design was based on Fig. S12B. *, P<0.05. **, P<0.01. ***, P<0.001. Error bars, mean±S.E.M.

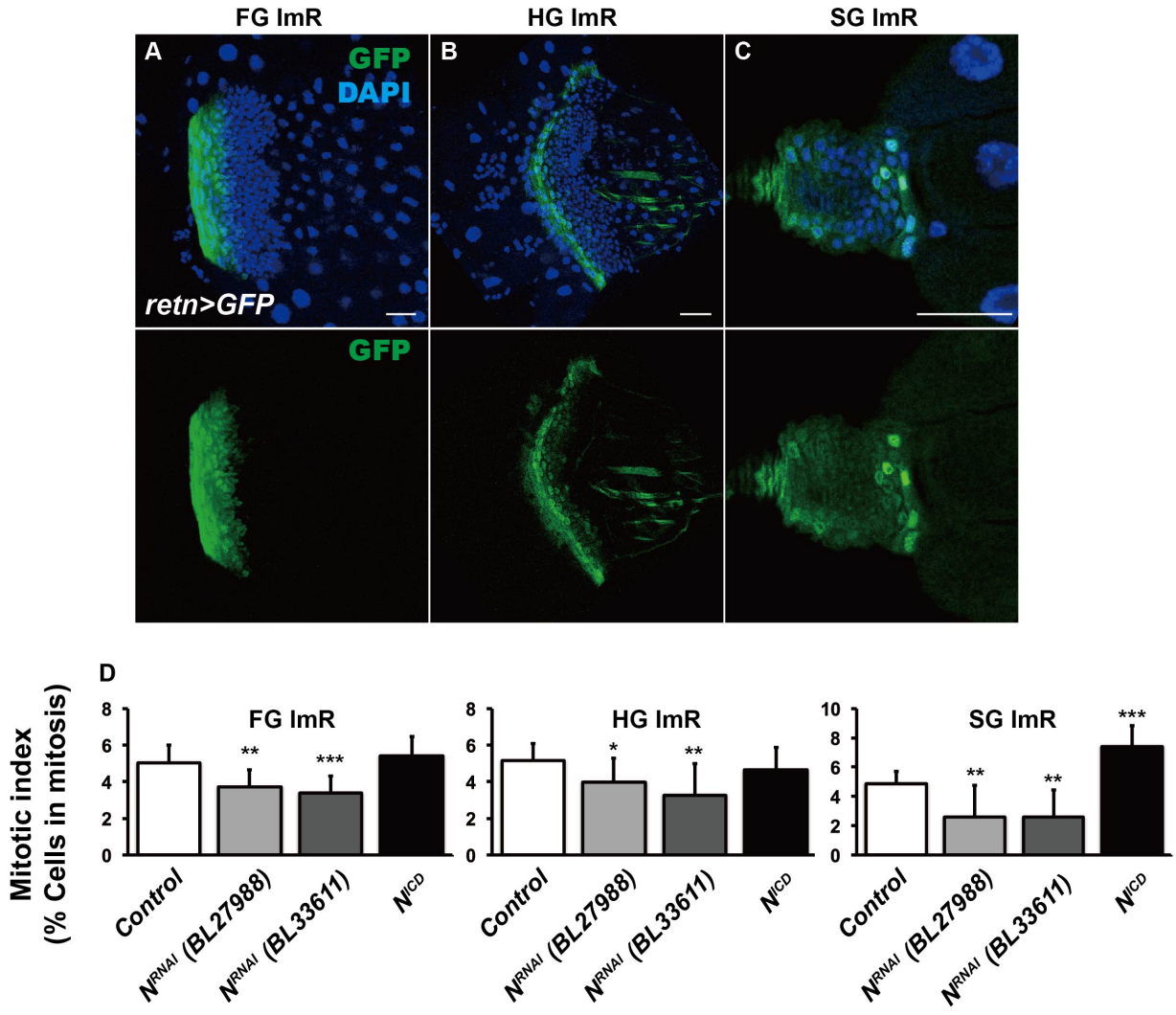

Fig. S5. *retn-Gal4* driver applied experiments.

(A-C) *retn-Gal4* driven GFP expression (green) in foregut imaginal ring (A), hindgut imaginal ring (B) and salivary gland imaginal ring (C) in third instar. Nuclei were labeled with DAPI (blue). Scale bar, 20μm. (D) Quantification of mitotic index in third instar. *, P<0.05. **, P<0.01. ***, P<0.001. Error bars, mean±S.E.M.

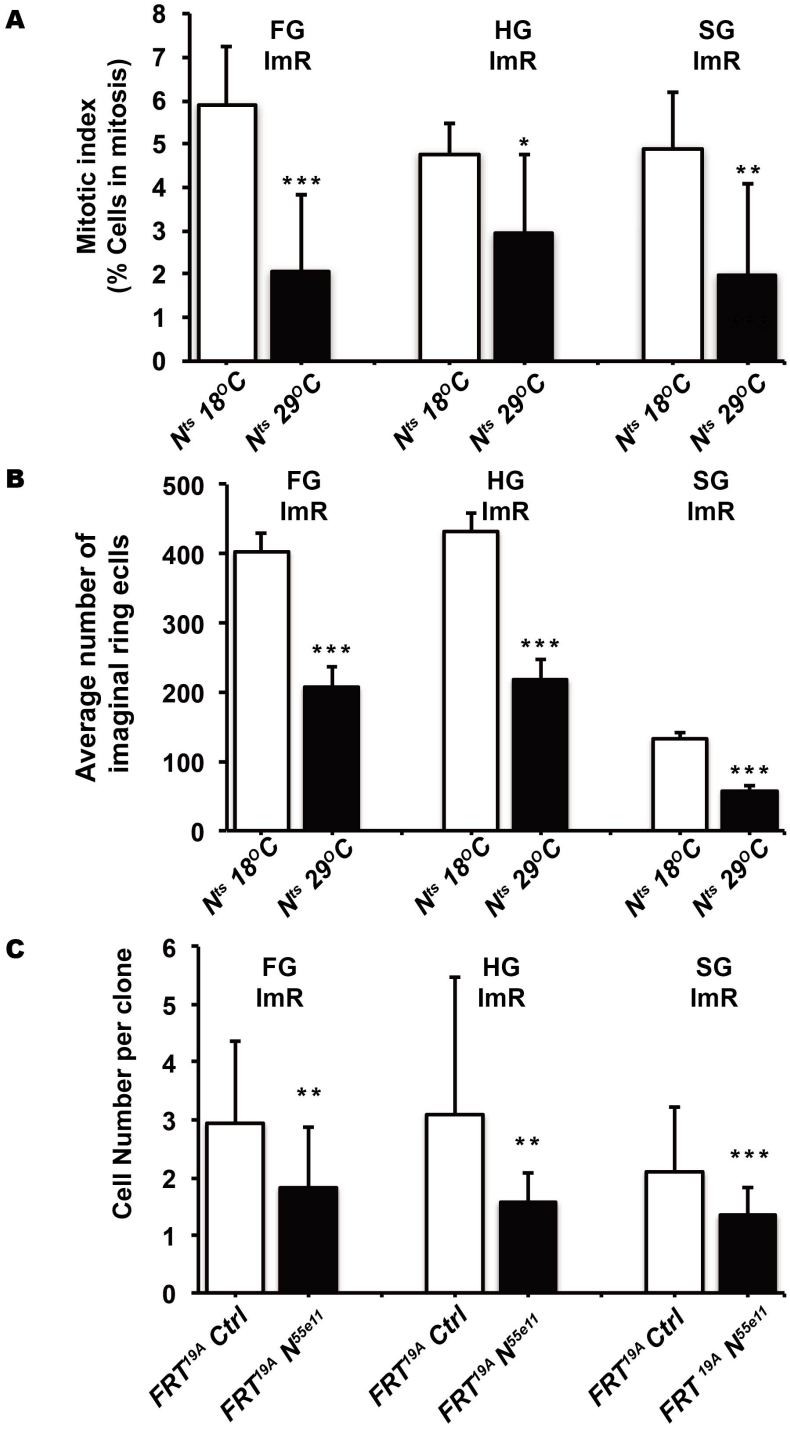

Fig. S6. *Notch* mutation analyses for imaginal ring cell proliferation.

(A-B) N^{ts} analyses. (A) Quantification of mitotic index at third instar. (B) Quantification for imaginal ring cell numbers at third instar. (C) MARCM clone of N^{55e11} mutation. The cell numbers in each clone at third instar were quantified. *, P<0.05. **, P<0.01. ***, P<0.001. Error bars, mean±S.E.M.

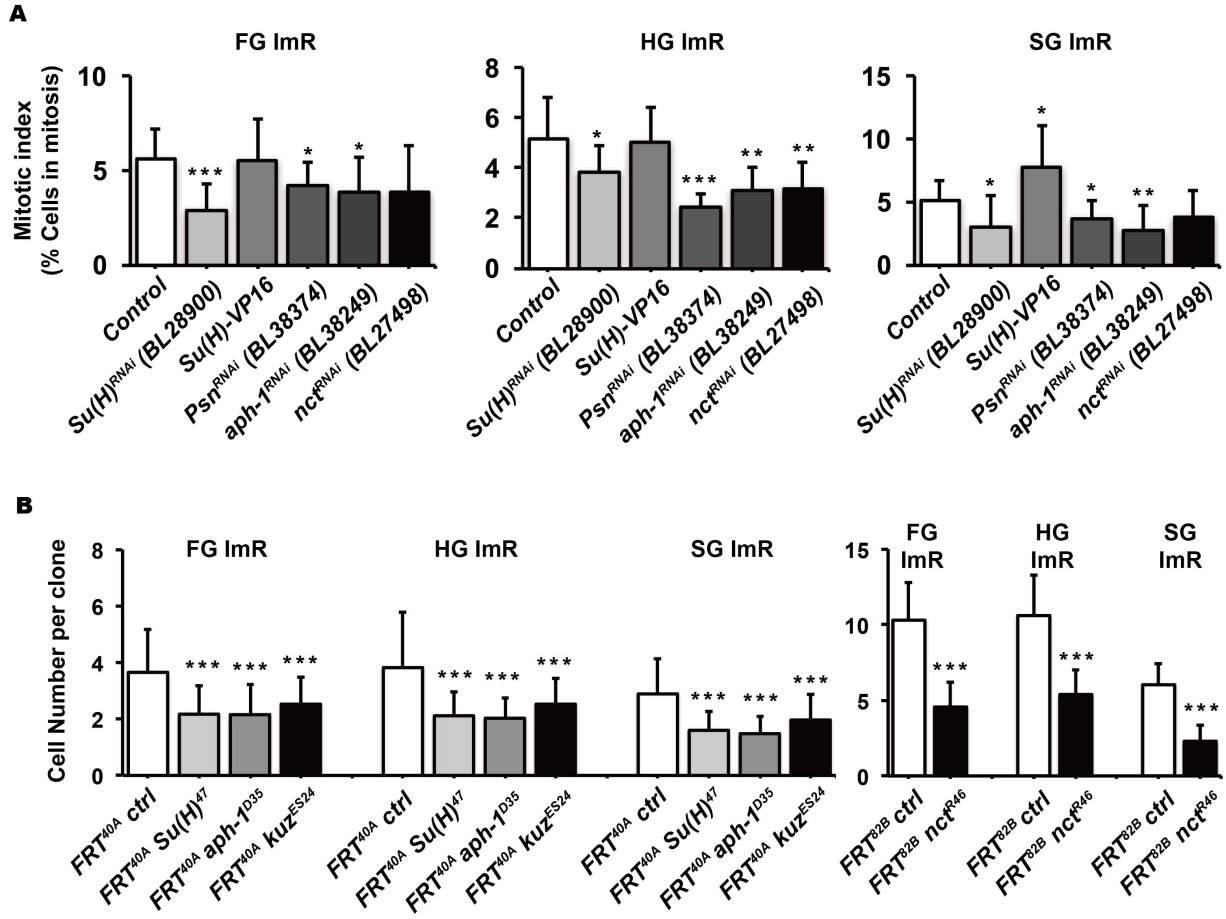

Fig. S7. Canonical Notch pathway is involved in cell proliferation in imaginal ring.

(A) Quantification of mitotic index at third instar. Canonical components in Notch pathway, *Su(H), Psn, aph-1 and nct*, knocked down by Act^{ts} caused lower cell proliferation. Overexpression of Su(H), active form of Su(H) by Act^{ts}, leaded higher mitotic activity. (B) Quantification of average cell number for MARCM-based clones at third instar. The size of clones with $Su(H)^{47}$, $aph\text{-}1^{D35}$, kuz^{ES24} or nct^{R46} mutations was reduced. *, P<0.05. **, P<0.01. ***, P<0.001. Error bars, mean±S.E.M.

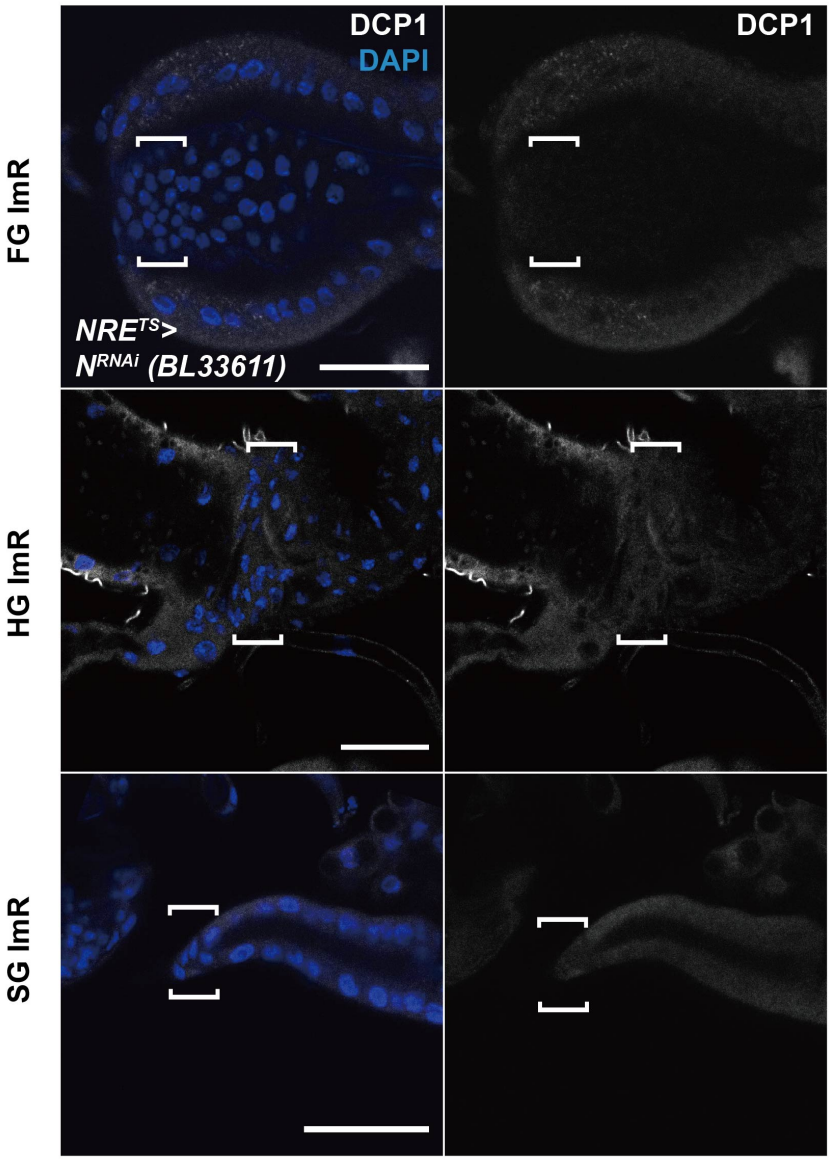

Fig. S8. *Notch* loss-of-function during young stages does not induce apoptosis.

(A-C) DCP1 staining (white) for apoptotic activity in foregut imaginal ring (A), hindgut imaginal ring (B) and salivary gland imaginal ring (C) in early first instar. DAPI labels nuclei (blue). Brackets indicate the regions of imaginal rings. Scale bar, 20μm.

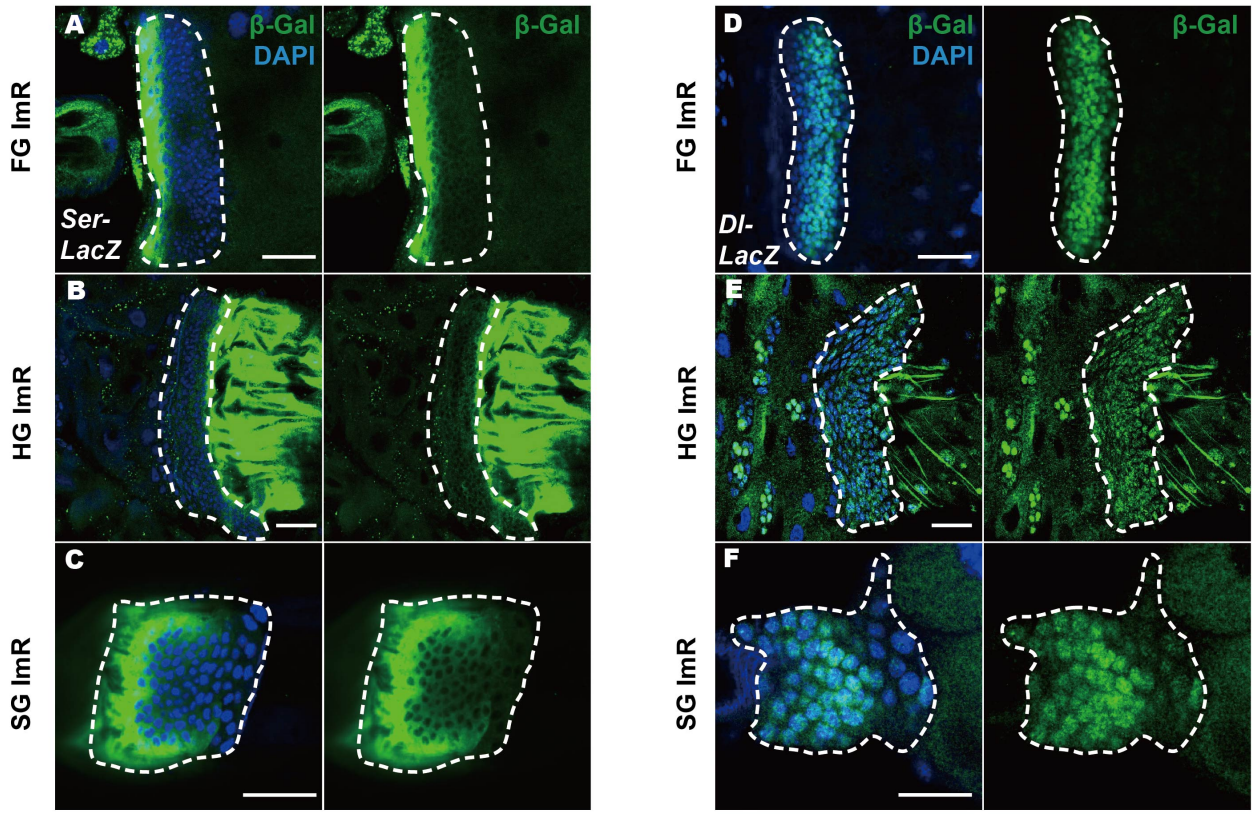

Fig. S9. *Ser-LacZ* and *Dl-LacZ* expression in imaginal ring of third instar larvae.

β-Gal antibody staining (green) for *Ser-LacZ* (A-C) and *Dl-LacZ* (D-F). (A and D) foregut imaginal ring; (B and E) hindgut imaginal ring; (C and F) salivary gland imaginal ring. Nuclei were labeled with DAPI (blue). Dashed lines indicate imaginal ring cells. Scale bar, 20μm.

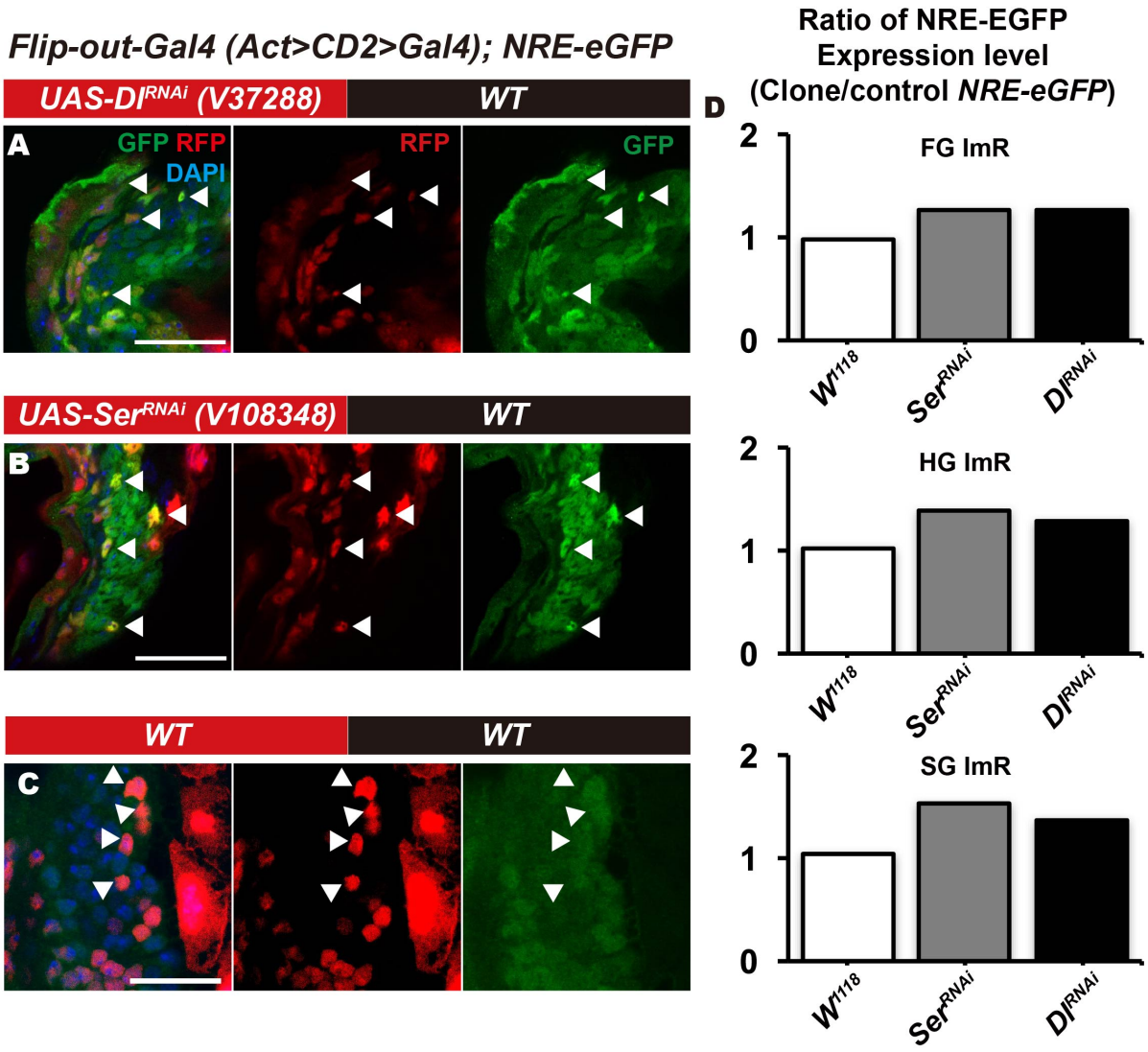

Fig. S10. *NRE-eGFP* expression is increased in small *Dl* or *Ser* loss-of-function clones in foregut imaginal rings at third instar larval stage.

Clones, labeled with RFP (red), were induced by Flip-out Gal4 driver with *Dl-RNAi* (A) or *Ser-RNAi* (B). Flip-out Gal4 control (C). *NRE-eGFP* indicated Notch activation (green). Nuclei were labeled with DAPI (blue). Arrowheads indicate single cell layer clones. Scale bar, 20μm. (G) The quantified ratio of eGFP intensity. The *NRE-eGFP* intensity in Ser or Dl loss-of-function and wildtype single-cell-layer clones was measured. The intensities of eGFP in clone cells were further divided by the intensities of eGFP from wildtype *NRE-eGFP* flies.

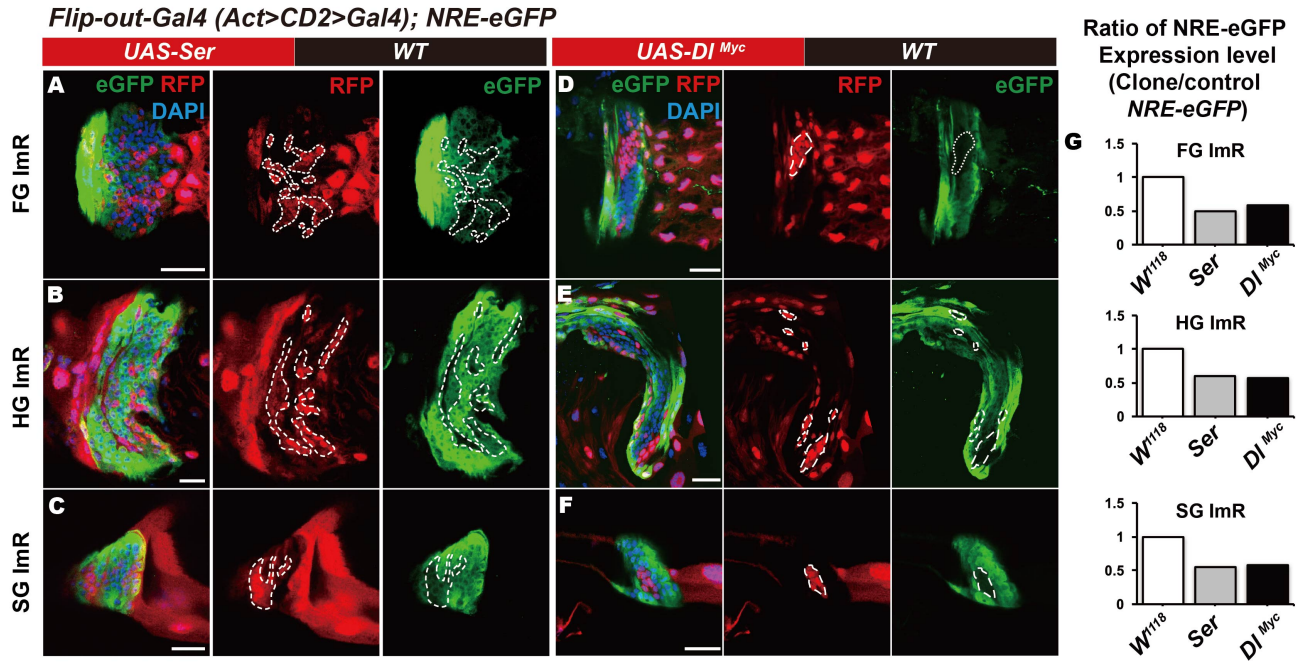

Fig. S11. *Cis*-inhibition occurs in imaginal rings.

Flip-out-Gal4 generated mosaic imaginal ring with clones overexpressing *Ser* (A-C) or Dl^{myc} (D-F). Third instar larvae were observed. (A and D) foregut imaginal ring; (B and E) hindgut imaginal ring; (C and F) salivary gland imaginal ring. Ligand expressing cells were labeled with RFP expression (red). *NRE-eGFP* indicated Notch activation (green). Nuclei were labeled with DAPI (blue). Dashed lines indicate clone cells. Scale bar, 20μm. (G) The quantified ratio of eGFP intensity. The *NRE-eGFP* intensity in Ser or Dl gain-of-function and wildtype clones was measured. The intensities of eGFP in clone cells were further divided by the intensities of eGFP from wildtype *NRE-eGFP* flies.

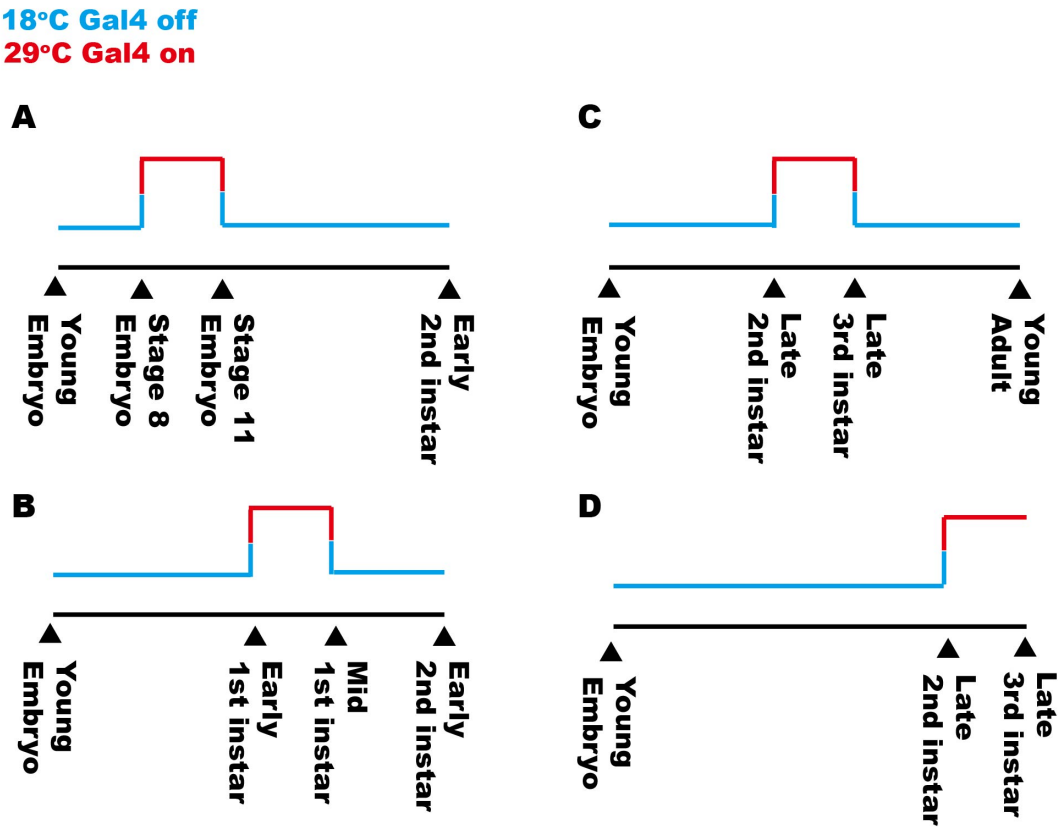

Fig. S12. Temperature shifting designs.

Blue lines for low rearing temperature (18°C, Gal4 is inactive) and red lines for high raising temperature (29°C, Gal4 is active). (A) Embryonic experiments. Flies only stayed at 29°C during embryonic stage 8-11 and were dissected at early-second instar. (B) Flies only stayed at 29°C during first instar and were dissected at early-second instar. (C) Flies only stayed at 29°C during late-second instar to late-third instar and were dissected at young adult stage. (D) Flies only stayed at 29°C during late-second instar to late-third instar and were dissected at late-third instar. For staging, wild-type flies reared at 25°C were used as standard for the comparisons. Embryonic features (Campos-Ortega and Hartenstein 2013) was applied for embryonic staging. Body size, spiracles and mouth hooks are used for larval staging (Shingleton).